Characterization of cross-spring pivots for micropositioning applications

K. Marković [*a], S. Zelenika [a]
[a] University of Rijeka, Faculty of Engineering & Centre for Micro and Nano Sciences and Technologies, Vukovarska 58, 51000 Rijeka, CROATIA

ABSTRACT

Compliant mechanisms gain at least part of their mobility from the deflection of flexible member. They are characterised by high precision, as well as no backlash and wear. Several analytical and numerical methods are used in this work to characterise the behaviour of compliant rotational mechanisms, known as cross-spring pivots, aimed at micropositioning applications. When ultra-high precision is required, the limits of applicability of approximated calculation algorithms have to be determined. The results obtained by employing these methods are thus compared with results obtained by using nonlinear finite element calculations tuned with experimental data reported in literature. The finite element model allows also considering the influence of lateral loads and of non-symmetrical pivot configurations where the angle or point of intersection of the leaf springs, or even the initial curvature of the springs, can be varied. The aim of this part of the work is to determine the influence of the cited design parameters on the minimisation of the parasitic shifts of the geometric centre of the pivot as well as on the minimisation of the variability of the rotational stiffness of the pivot so as to ensure its stability. The obtained results allow therefore determining design solutions applicable in ultra-high precision micropositioning applications, e.g. in the field of production or of handling and assembly of MEMS.

Keywords: cross-spring pivots, micropositioning, FEA modelling, design parameters, parasitic shifts, stiffness & stability

1. INTRODUCTION

Compliant mechanisms are an alternative to sliding and rolling mechanisms when transfer of motion, energy and power is to be attained. Gaining their mobility from the deflection of flexible members, often in the form of spring-strips, compliant mechanisms are characterised by high precisions, accuracies and resolutions, possibility of monolithic manufacturing (allowing thus design-for-no-assembly to be achieved), reduced costs as well as absence of backlash and wear. What is more, the main sources of errors in these devices are systematic and therefore simple control laws can be used. Owing to these advantages, compliant mechanisms are thus widely used in mechanical engineering design, precision engineering, the micro- and nanotechnologies, metrology, ICT, aerospace technologies, astrophysics, automotive industry, machine tools, biomedical applications, robotics, but also in several every day's applications [1-7].

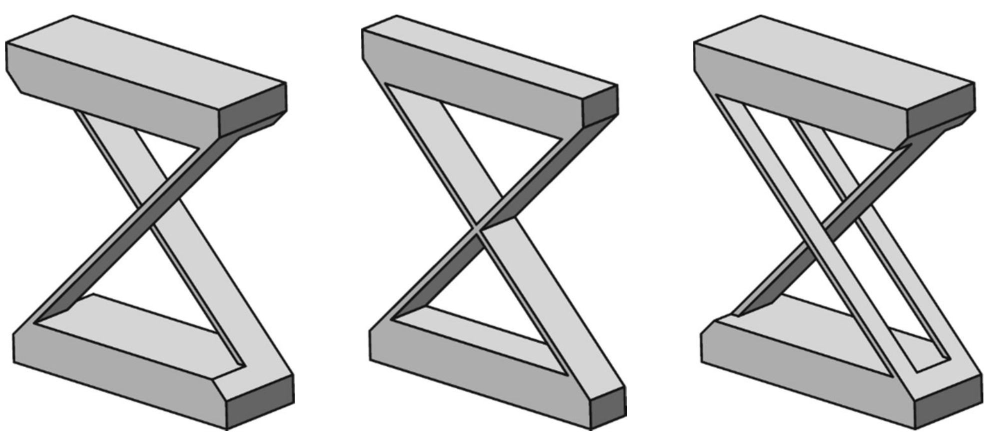

Figure 1. Different design configurations of a symmetrical cross-spring pivot.

[*] kristina@riteh.hr; phone +385 – (0)51 651535; fax +385 – (0)51 651416; www.riteh.uniri.hr & www.cmnzt.uniri.hr

Smart Sensors, Actuators, and MEMS VII; and Cyber Physical Systems, edited by José L. Sánchez-Rojas, Riccardo Brama, Proc. of SPIE Vol. 9517, 951727 · © 2015 SPIE
CCC code: 0277-786X/15/$18 · doi: 10.1117/12.2178490

A compliant mechanism used to accomplish a rotational joint is often referred to as the cross-spring pivot (Fig. 1). It is characterised by a marked compliance along the ‘in plane’ rotational degree of freedom (DOF) and high stiffness (order of magnitudes higher than that of the main DOF) along the secondary (transversal) DOFs. As shown in Fig. 2, cross-spring pivots consist of a rigid body B connected by using spring-strips 1 and 2, generally intersecting at their midpoints, with a movable block A. In the usual configuration, the used spring-strips have the same length L, width b and thickness t (Fig. 2a) and are made of the same spring material with a high yield strength $\sigma_{0.2}$ – to – Young ’s modulus E radio. When loaded with a pure couple M, the cross-spring pivot allows therefore the block A to rotate, via the deflection of the spring-strips, with respect to the fixation B (Fig. 2b). For larger rotation angles θ, however, the ‘geometrical’ centre of the pivot O moves to point O’ defined by the tangents to the fixed ends of the strips in the movable block, giving hence rise to a parasitic shift of amplitude d and phase φ. This parasitic motion is, obviously, detrimental to the precision of the analysed mechanisms. What is more, when loaded with transversal forces H and V, the range of stability of the mechanism can be limited, since buckling can occur in one or both spring-strips inducing a negative restoring moment for the whole mechanism, i.e. the occurrence of its negative rotational stiffness [8-11].

In order to assess the influence of these harmful effects on the performances of cross-spring pivots, the equilibrium of loads and internal reactions of the whole mechanism (Fig. 2b) has to be considered. This can be brought down to the analysis of the stress-strain behaviour i.e. the equilibrium of forces and torques acting on the single spring-strips. In literature are available several analytical and experimental approaches used so far for this task [8-20].

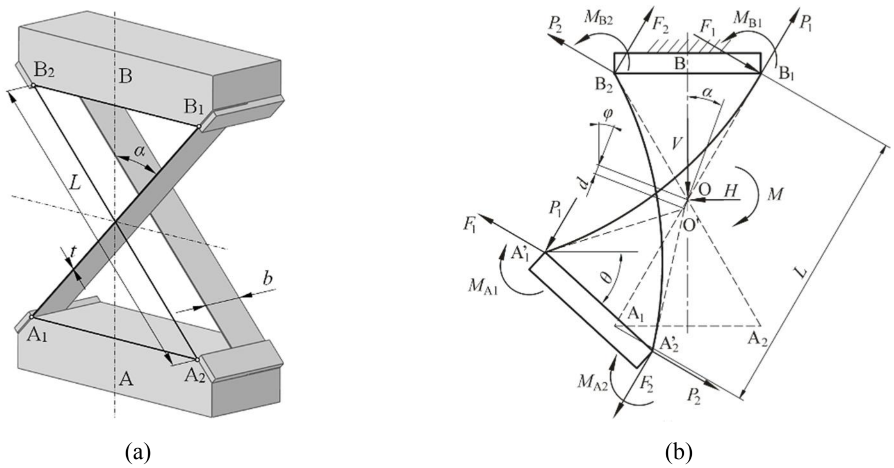

Figure 2. Characteristic dimensions of the cross-spring pivot (a) and schematics of the pivot in deformed position (b).

The aim of this work is to establish the limits of applicability of the diverse analytical approaches available in literature for the analysis of the behaviour of cross-spring pivots as well as to determine an optimised design configuration that allows minimising the parasitic shifts and the variability of the rotational stiffness, while preserving the stability of the mechanism, its simple design and its reliability.

In section 2 of the paper, a nonlinear finite element model (FEM) of the pivot, matching the experimental measurements used to assess its behaviour, is hence developed by using the ANSYS® FEM software package. This numeric model is then used in section 3 to assess the accuracy limits of the analytical approaches used so far in literature to model the behaviour of the analysed class of mechanisms. Various design configurations of the cross-spring pivot are then analysed in section 4 by employing the developed FEM algorithms and design solutions that minimise parasitic shifts while guaranteeing the stability of the mechanism with minimal variability of its rotational stiffness even in the presence of lateral loads, are identified. These design configurations are hence applicable in ultra-high precision micropositioning applications, e.g. in the field of production or of handling and assembly of MEMS.

2. NUMERICAL MODEL

Using the commercial ANSYS® FEM package that enables nonlinear large deflection analyses of cross-spring pivots, a finite elements analysis (FEA) numerical model is developed. BEAM189 quadratic 3D beam three-node elements with six degrees of freedom at each node, based on Timoshenko’s beam theory [21], are used to create an idealization of the threedimensional cross-spring pivot structure (Fig. 3a). These elements support nonlinear analyses including large (geometrically nonlinear) deflections. The FEA model allows then the amplitude d and phase φ of the parasitic shifts of the geometric centre of the pivot in its deformed position to be easily determined by following the coordinates of the free end of a thin stiff beam $\overline{OA_3}$ (Figures 3b & 3c). The dimensions and material of the spring-strips used in the FEA model are those considered in the most recent experimental measurements reported in [8], i.e. the spring-strips' length, width and thickness are, respectively, L = 115 mm, b = 15 mm and t = 0.5 mm, the angle between the spring-strips is $2\alpha = 90°$, while Young's modulus of the spring-strips' material (a beryllium-copper alloy) is E = 131000 N/mm^2.

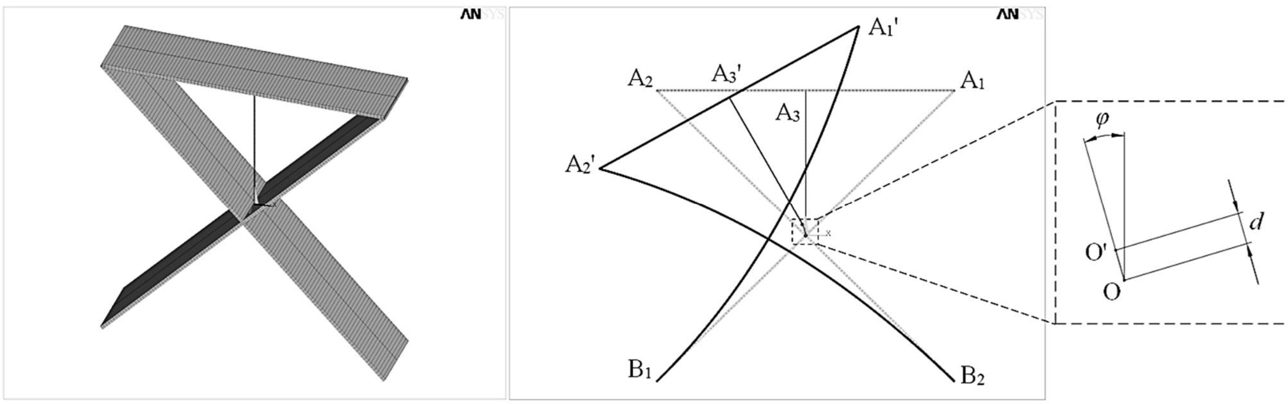

(a) (b) (c)

Figure 3. Meshed finite element model (a), deformed FEM of the cross-spring pivot (b) and its parasitic shift (c).

In order to assess the applicability of the developed numerical model in predicting the stress-strain behaviour of the considered class of mechanisms, the results obtained by using this FEA model and then compared with results of experimental measurements reported in literature for pivots loaded with a pure couple M [8, 11, 15, 18-20]. The comparison, shown in Fig. 4, is performed in terms of the normalized parasitic shift amplitudes d/L versus pivots' rotation θ. It can thus be seen that FEA results match excellently with the results of recently performed experimental measurements based on a Michelson-type laser Doppler interferometric system, characterised by high accuracies and small intervals of uncertainty [8]. In fact, the differences between the interferometric measurements and the FEM analyses are smaller than 2% in the whole considered range of pivot rotations ($0 < \theta \leq 30°$). Although the measurement techniques used in other published works allow the general trends of the parasitic shifts' magnitudes to be identified, they are characterized by higher uncertainties (in these cases, styluses, pointers or measuring and toolmakers' microscopes were used), and are thus less relevant. FEA results obtained for parasitic shifts' phases φ, as well as for the rotational stiffness of the pivot, are also matching well with the experimental measurement results, confirming that the developed numerical model is a computationally efficient and accurate tool for the prediction of the behaviour of cross-spring pivots.

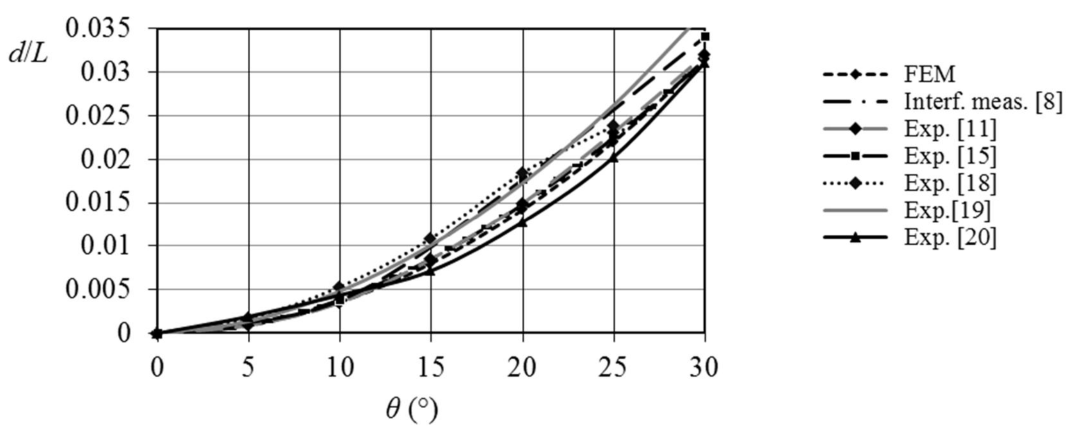

Figure 4. Comparison of normalized parasitic shift amplitudes d/L obtained via the FEA model with experimental results.

3. ANALYTICAL METHODS

The developed and verified FEA model is used next to assess, depending on the required degrees of accuracy, the limits of applicability of the analytical methods proposed in literature for modelling the behaviour of cross-spring pivots loaded with a pure couple *M* [8-10, 12-17]. The results obtained via the numerical analysis are thus compared with those obtained by using:

- the Elastica approach (EL) that takes into account the exact expression for the curvature of the spring-strips in the domain of large (geometrically nonlinear) deflections [9, 12];
- approaches based on approximated expression for the curvature of the beam where the influence of the axial components of the load on spring-strips' bending is still considered, but the square of the derivative in the curvature formula is neglected (AC) [8, 10];
- approaches based on the pseudo-rigid-body model (PRBM) where an equivalent mechanism constituted by rigid members hinged via suitably positioned joins comprising torsional springs, so as to generate the same load-displacement characteristic as the original (in this case cross-spring pivot) mechanisms, is studied – in particular, in this work are considered PRBM configurations in the four bar and pin joint arrangements analysed in [13], as well as in the configuration where each spring-strip is substituted with a rigid bar with two pin joints but, as proposed in [14], only one of these is coupled with a torsional spring of equivalent stiffness;
- approaches based on a kinematic model (KM) of the cross-spring pivot [15];
- geometrical methods (GM) as proposed in [16] or those based on a simple hinged frame with four rigid bars [17].

The comparison of the results obtained with the cited approaches is reported in Fig. 5a in terms of the normalised parasitic shift amplitudes d/L, and on Fig. 5b in terms of the couple *M* needed to achieve the rotation of the cross-spring pivot for a given rotation angle θ. The comparison of the results is easier if the differences $\Delta d/L$ and ΔM of the results obtained with the various analytical approaches with respect to the FEM values are reported (secondary vertical axes in Fig. 5).

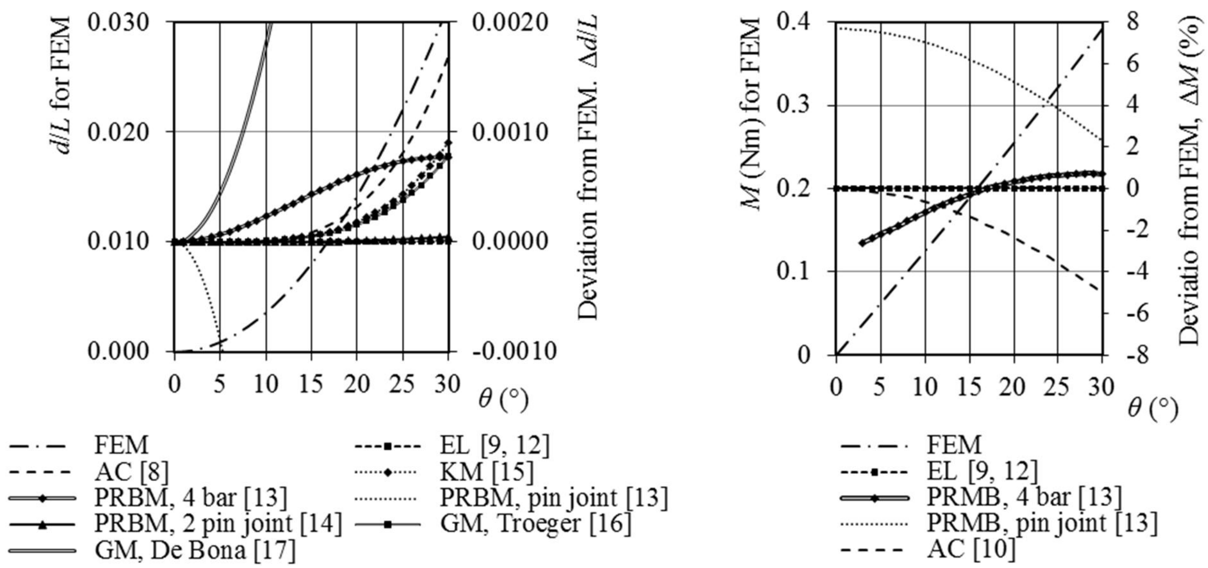

(a) (b)

Figure 5. Comparison of FEM and results of various analytical methods in terms of normalised parasitic shift amplitudes (a) and couples (b) vs. rotation angle θ.

From the curves depicted in Fig. 5a it can be observed that the EL results of the parasitic shift amplitude, which take into account the nonlinear effects, practically coincide with FEM analysis results even for large rotation angles of the pivot. The EL approach is, however, computationally intensive due to the presence of elliptic integrals that have to be iteratively evaluated in the calculation routine [12]. Amongst the approximate analytical methods, the two pin joints PRBM approach [14] results in the smallest deviations. The AC, KM and GM approaches suggested, respectively, in [8], [15] and [16], are in good agreement with FEA results for rotation angles θ smaller than 15°. Finally, the PRBM results obtained by using the approaches proposed in [13], as well as the GM results according to [17], allow only a first-degree approximation of the real behaviour of cross-spring pivots loaded with a pure couple.

On the other hand, from the comparison of the couples needed to induce a given rotation θ of the cross-spring pivot depicted in Fig. 5b, it can be established that the EL results are again coinciding with FEA results in the whole range of considered rotations. The results obtained by employing the AC approach suggested in [10] result in errors that increase for increasing rotation angles θ, whereas the four bar PRBM approach [13] gives relatively good results for rotation angles θ larger than 10°. Results obtained by using the pin joint [13] arrangement of the PRBM result in considerable errors, while the other considered analytical approaches do not allow the entity of the couple M to be calculated.

4. INFLUENCE OF DESIGN PARAMETERS

By using the developed FEM algorithms, effects induced by the variation of design parameters on the values of the parasitic shifts, the rotational stiffness and the stresses occurring for diverse design configurations of cross-spring pivots, which could hardly (if at all) be assessed with the Elastica analytical approach [8], can also be thoroughly analysed. In this work are considered the variations of:

- the angle α defining the inclination of the spring-strips with respect to the vertical axis of the cross-spring pivot (Fig. 6a);
- the longitudinal position of the intersection of the spring-strips defined by the parameter λ (Fig. 6a);
- the initial curvature of spring-strips defined by the angles γ_1 and γ_2 at their fixations in, respectively, the fixed and the movable block (Fig. 6b);

as well as design configurations where:

- the spring-strips are joined in pivots' geometrical centre O so as to create a monolithic configuration of the mechanisms
- and additional external transversal loads (H and V in Fig. 2b) are applied to the pivot.

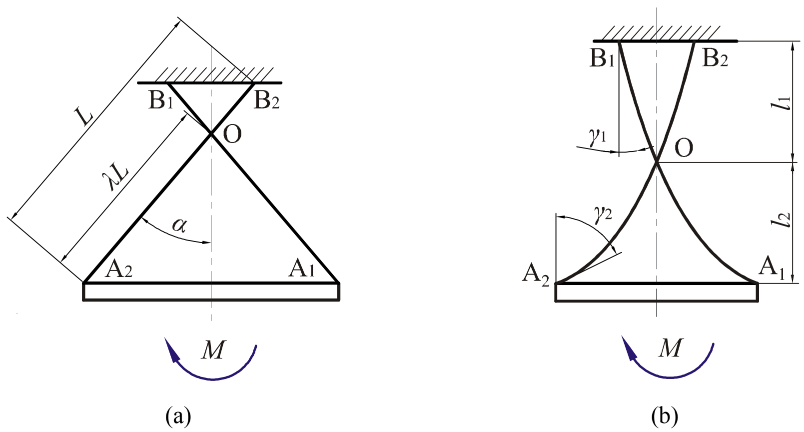

Figure 6. Variants of the cross-spring pivot design.

In Fig. 7 is shown how the change of the inclination angle α of the spring-strips with respect to the vertical axis affects the behaviour of the cross-spring pivot, determined via nonlinear FEA. It is thus visible that an increase of α induces a rise of the values of the normalized parasitic shift amplitudes d/L (Fig. 7a), a marked increase of rotational stiffness K ($K = M/\theta$ – Fig. 7b) and an almost linear increase of the stresses σ_{max} in the fixations of the spring-strips (Fig. 7c).

On the other hand, as depicted in Fig. 8, a variation of the position of the geometrical centre of the pivot O defined via the parameter λ of Fig. 6a, for a fixed inclination $\alpha = 45°$of the spring-strips, causes a substantial variation of the parasitic shift amplitudes d/L (Fig. 8a), of rotational stiffness K (Fig. 8b) and of the stresses σ_{max} at the fixed ends of the spring-strips (Fig. 8c). It is important to be noticed here that, for a design configuration for which the geometric parameters $\lambda \approx 0.13$ and $\alpha = 45°$, the parasitic shifts become negligible even for large rotation angles θ, at the expense, however, of a large increase of rotational stiffness and the stresses. Contrary to what is generally reported in literature, where it is stated that the λ value that minimises the parasitic shifts is constant [14, 22-24], the value of λ for which the parasitic shifts will be minimised will, however, change depending on the inclination α of the spring-strips and on the entity of pivot's rotation θ.

A similar nonlinear numerical analysis of cross-spring pivot configurations with an initial curvature of the spring-strips (Fig. 6b) allows establishing that this configuration induces significantly larger parasitic shifts than the conventional pivots' configurations of Fig. 2, accompanied by a large increase of rotational stiffness and of the stresses.

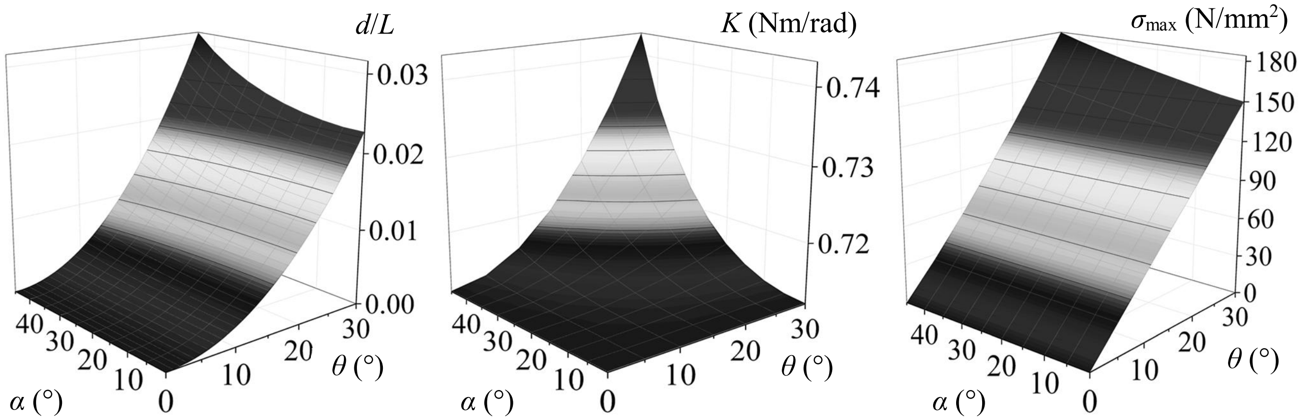

(a) (b) (c)

Figure 7. Change of normalised parasitic shift amplitudes (a), rotational stiffness (b) and stresses at spring-strips' fixed ends (c) versus rotation θ depending on the inclination α of the springs.

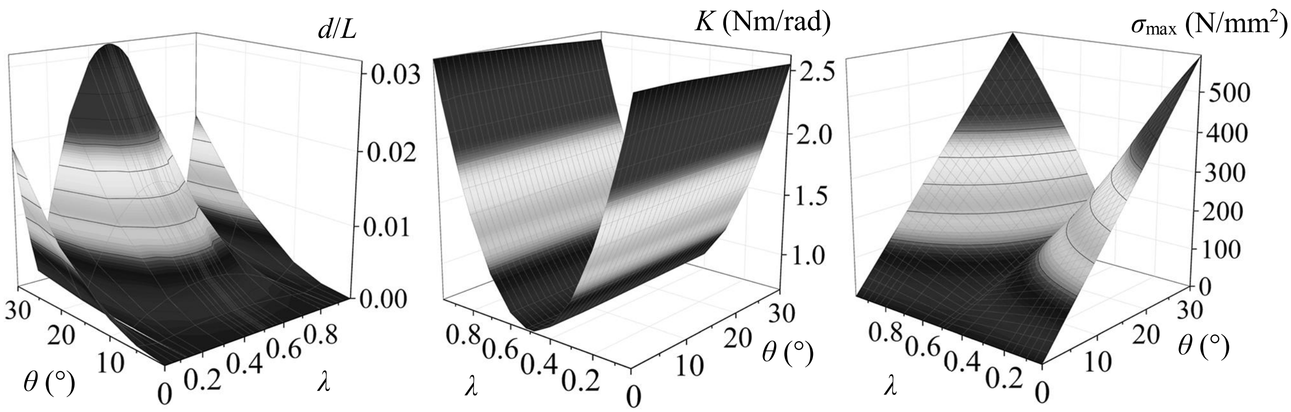

(a) (b) (c)

Figure 8. Change of normalised parasitic shift amplitudes (a), rotational stiffness (b) and stresses at spring-strips' fixed ends (c) versus rotation θ depending on parameter λ for a design configuration with $\alpha = 45°$.

When compared to a conventional pivot's configuration of Fig. 2, a monolithic configuration of the cross-spring pivot, where the spring-strips are joined in the pivot geometric axis O and considering variable spring-strips' inclinations α, leads to, as shown in Fig. 9, a decrease of parasitic shifts of up to even 10 times (!), even though at the expense of a conspicuous increases of pivot's stiffness (up to five times) and of the stresses induced in the spring-strips (up to four times). It would seem that the "butterfly" monolithic configuration suggested in literature [25], although complex and technologically cumbersome, could alleviate this situation by lowering further the parasitic shifts while mitigating the increase of stiffness and stresses.

Finally, a nonlinear FEM analysis of the influence of additional external loads on the variability of rotational stiffness and on the entity of the parasitic shifts is also performed. Physically, the influence of a horizontal transversal force H can be seen as a mere superposition to the effect of the couple M. In Fig.10 are therefore shown the results of numerical analyses of the influence of the vertical external load V (acting along with M) on the normalized rotational stiffness $KL/(EI)$ of the cross-spring pivot when its characteristic angle is $\alpha = 45°$. It can thus be seen that a compressive vertical force V_C loading the pivot narrows substantially the stability range of the pivot. With respect to the conventional pivot's configuration of Fig. 2, this loading condition induces, in fact, also an increase of rotational stiffness and a decrease of parasitic shift amplitudes. On the other side, a tensile external load V_T can induce a decrease of rotational stiffness and an increase of parasitic shift amplitudes. By varying the position of the intersection of the spring-strips along their lengths, tensile loads induce then a broadening of the stability range of the pivots (that where the stiffness is positive), so that, as visible in Fig. 10, the cross-spring pivot configuration with $\lambda = 0.1$ loaded with a tensile external force allows achieving a slight variation of rotational stiffness and a small parasitic shift for a range of vertical loading where $V_T L^2/(EI) \leq 30$. A design configuration for which the geometry of the pivot is such that $\lambda \approx 0.13$ (i.e. the one for which, as shown in Fig. 8, the parasitic shift amplitudes are negligible), permits accomplishing a very small variation of rotational stiffness as long as $|VL^2/(EI)| \leq 10$ (i.e. irrespective of the orientation of vertical loads – see zoomed region of Fig. 10).

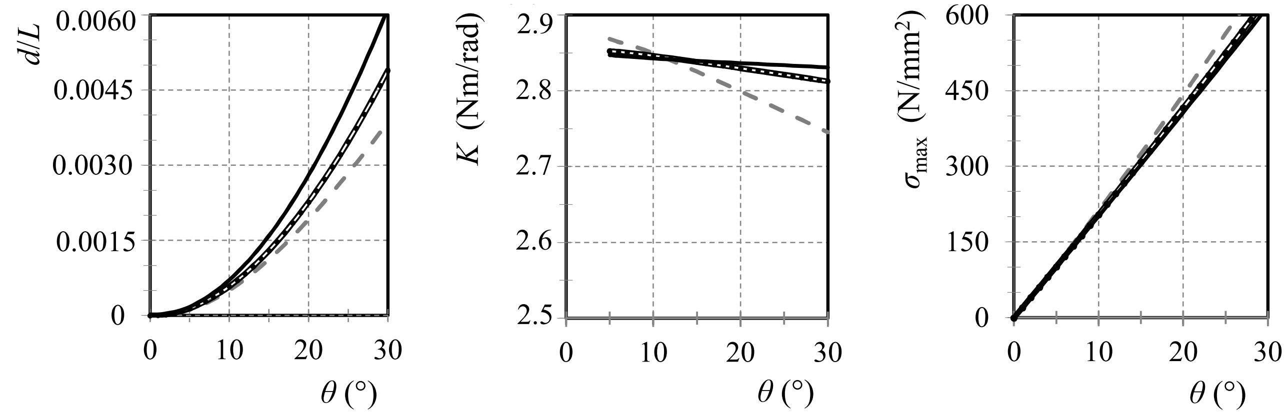

(a) (b) (c)

Figure 9. Change of d/L (a), K (b) and σ_{max} (c) versus rotation θ for a monolithic pivots' configuration with $\alpha = 15°$ (dashed line), $\alpha = 30°$ (compound line) and $\alpha = 45°$ (solid line).

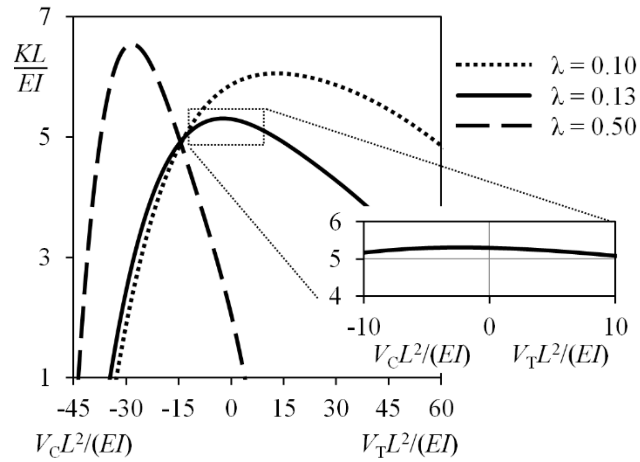

Figure 10. Rotational stiffness depending on vertical loads for various values of the geometric parameter λ when $\alpha = 45°$.

5. CONCLUSIONS

Results obtained via a suitably configured nonlinear FEA model are compared in this work to experimental data on the behaviour of cross-spring pivots aimed at ultra-high precision and microsystems technologies application, confirming its validity. Numerical FEA is then used to determine the range of applicability of the analytical methods available in literature, allowing to establish that, in the case of pivots loaded merely with a pure couple, only the nonlinear and computationally demanding Elastica approach is suitable to model the behaviour of the pivots when high precisions and/or large rotation angles are aimed for. Nonlinear FEM, which allows quick and reliable study of various design configurations of the pivot, is subsequently also used to study thoroughly the influence of design parameters (various geometric and loading conditions) on the minimization of parasitic shifts and of the variability of the stiffness of the studied class of mechanisms. It is hence established that a design arrangement of the cross-spring pivot with $\lambda \approx 0.13$ and $\alpha = 45°$ allows ultra-high precisions to be achieved since it is characterized by negligible parasitic shifts even for large pivot rotations, while allowing to maintain the stress levels in the spring-strips well within the allowable limits. λ values that allow minimising parasitic shifts will, however, depend on spring-strips' inclination α, the range of rotations θ, as well as on the transversal forces loading the pivot. In fact, pivot's configuration with $\lambda \approx 0.13$ and $\alpha = 45°$ is characterized not only by small parasitic shifts, but also by a slight variations of rotational stiffness as long as the transversal loads, acting on the pivot alongside the pure couple, are of limited entity. For intersection points close to one of the pivots' blocks (i.e. for values $\lambda < 0.5$), vertical tensile forces loading the pivot seem in any case to have a positive effect on its stability. A configuration with $\lambda = 0.1$ allows thus achieving small rotational stiffness variations and small parasitic shifts for a rather large span of tensile vertical loads. It can be thus concluded that cross-spring pivot design configurations with the values of the λ parameter in the $0.1 \leq 0.13$ range are applicable in a broad range of ultra-high precision micropositioning applications such as, for instance, in the field of production or of handling and assembly of MEMS.

ACKNOWLEDGEMENTS

This work is partially supported by the University of Rijeka project nr. 13.09.1.2.09.

REFERENCES

[1] De Bona, F. and Zelenika, S., "Design of Compliant Micromechanisms," in: De Bona, F. and Enikov, E. T. (ed.), [Microsystems Mechanical Design], Springer. Wien & New York, 119-134 (2006).
[2] Howell, L. L., [Compliant Mechanisms], Wiley & Sons, New York (2001).
[3] Jones, R. V., "Some uses of elasticity in instrument design," J. Sci. Instr. 39, 193-203 (1962).
[4] National Physical Laboratory, "Notes on Applied Science No. 15," London – H. M. Stationary Office (1956).
[5] Pavlović, N. D. and Pavlović, T. D., [Gipki mehanizmi], U. of Niš (2013).
[6] Smith, S. T., [Flexures: Elements of Elastic Mechanisms], Gordon & Breach Sci. Publ., Amsterdam (2000).
[7] Smith, S. T. and Chetwynd, D. G., [Foundations of Ultraprecision Mechanism Design], Gordon & Breach Sci. Publ., Amsterdam (1992).
[8] Zelenika, S. and De Bona, F., "Analytical and experimental characterisation of high-precision flexural pivots subjected to lateral loads," Prec. Eng. 26, 381-388 (2002).
[9] Haringx, J. A., "The Cross-Spring Pivot as a Constructional Element," Appl. Sci. Res. A1/4, 313-332 (1949).
[10] Wittrick, W. H., "The theory of symmetrical crossed flexure pivots," Aust. J. Sci. Res. A1/2, 121-134 (1948).
[11] Siddall, G. J., [The Design and Performance of Flexure Pivots for Instruments], M.Sc. Thesis, U. Aberdeen (1970).
[12] De Bona, F. and Zelenika, S., "A generalized Elastica-type approach to the analysis of large displacements of spring-strips," Proc. Instn. Mech. Engrs. C211, 509-517 (1997).
[13] Jensen, B. D. and Howell, L. L., "The modelling of cross-axis flexural pivots," Mech. Mach. Theor. 37, 461-476 (2002).
[14] Pei, X., Yu, J., Zong, G. and Bi, S., "An effective pseudo-rigid-body method for beam based compliant mechanisms," Prec. Eng. 34, 634-639 (2010).
[15] Wuest, W., "Blattfedergelenke für Messgeräte," Feinwerktechnik 54/7, 167-170 (1950).
[16] Troeger, H., "Considerations in the Application of Flexural Pivots," Aut. Contr. 17/4, 41-46 (1962).
[17] De Bona, F. and Zelenika, S., "Characterization of high precision parallel spring translators," in: Ikawa, N., Shimada, S., Moriwaki, T., McKeown, P. A. and Spragg, R. C. (ed.), [International Progress in Precision Engineering], Butterworth-Heinemann, Boston, 761-772 (1993).
[18] Hildebrand, S, "Obliczanie i zachowanie sie w pracy sprezyn krzyzowych," Pom.-Aut.-Kontr. 11, 501-508 (1958).
[19] Nickols, L. W. and Wunsch, H. L., "Design Characteristics of Cross-Spring Pivots," Eng., 473-476 (1951).
[20] Young, W. E., "An Investigation of the Cross-Spring Pivot," ASME J. Appl. Mech. 11, A113-A120 (1944).
[21] Ansys Inc. [ANSYS 13.0 Mechanical APDL] (2014).
[22] Wittrick, W. H., "The properties of crossed flexure pivots, and the influence of the point at which the strips cross," Aer. Quart. 2, 272-292 (1951).
[23] Hongzhe, Z. and Shusheng, B., "Accuracy characteristics of the generalized cross-spring pivot," Mech. Mach. Theor. 45, 1434-1448 (2010).
[24] Goncalves Jr., L. A., Bitencourt, A. C. P., Theska, R. and Lepikson, H. A., "Characterization of the elasto – kinematic behavior of generalized cross – spring bearings," Proc. 58th Ilmenau sci. coll., Ilmenau, Germany (2014).
[25] Henein, S., Spanoudakis, P., Droz, S., Myklebust, L. I. and Onillon, E., "Flexure pivot for aerospace mechanisms," Proc. 10th Eur. Space Mech. & Tribol. Symp., Noordwijk, Netherlands (2003).